Ni–W diffusion barrier: Its influence on the oxidation behaviour of a β-(Ni,Pt)Al coated fourth generation nickel-base superalloy

E. Cavaletti [a,*], S. Naveos [a], S. Mercier [a], P. Josso [a], M.P. Bacos [a], D. Monceau [b]

[a] ONERA, Metallic Materials and Structures Department, 29, Avenue de la Division Leclerc, BP 72, 92320 Châtillon, France
[b] Institut Carnot CIRIMAT, Université de Toulouse, ENSIACET, 118 route de Narbonne, 31077 Toulouse Cedex 04, France

A B S T R A C T

A Ni–W base diffusion barrier (DB) has been developed to limit interdiffusion between a fourth generation Ni-base superalloy (MCNG) and a Pt-modified nickel aluminide bondcoat. After long term oxidation, the DB layer permits to reduce the Al depletion in the coating and to delay the phase transformations in the coating. But despite this result, the oxidation behaviour of the system with DB is slightly worse than without the DB. This difference may be caused by the addition of S and/or W in the coating of the system with the DB. The DB layer also delays the Secondary Reaction Zone (SRZ) formation. Nevertheless, the propagation of the SRZ is similar in systems with and without a DB, with growth kinetics which are driven by interdiffusion.

Keywords:
Superalloy
Bondcoat
Diffusion barrier
Interdiffusion
Oxidation
Secondary reaction zone

1. Introduction

Thermal Barrier Coating (TBC) systems are the most advanced protection for high pressure turbine blades. TBC systems currently in use are composed of an outer 8 wt.%-Y_2O_3/ZrO_2 ceramic layer insulating the inner parts from the hot combustion gas, an intermediate Pt-modified nickel aluminide β-(Ni,Pt)Al oxidation protective coating, and an inner Ni-base superalloy which is the structural part of the system. At high temperature, interdiffusion occurs between the Ni-base superalloy and its nickel aluminide protective coating, and degrades the complete system [1]. Firstly, diffusion of some superalloy elements through the coating decreases the protective oxide scale adhesion. Secondly, oxidation and diffusion cause Al depletion in the coating, which leads to phase transformations [2,3] and affects the lifetime of the system. Finally, in third or fourth generation Ni-base superalloys coated with β-(Ni,Pt)Al, interdiffusion leads to the formation of detrimental and fast growing Secondary Reaction Zones (SRZ) [4,5]. In these SRZ, discontinuous precipitations transform the single-crystal γ/γ′ superalloy in a weaker polycrystal composed of γ and TCP phases (σ, P or μ) in a γ′ matrix. These zones degrade the mechanical properties of the system by reducing its bearing load section.

To limit interdiffusion between the Ni-base superalloy and its protective coating, diffusion barriers (DB) have been developed [6–8]. But the fabrication of these DB is complex and often requires a Ni deposition step before the aluminizing process. To simplify fabrication, a DB based on a Ni–W electrolytic coating was developed at ONERA [9]. A previous study [10] has confirmed that this coating, followed by a 16 h thermal treatment at 1100 °C, permits:

- the creation of a DB layer thanks to the precipitation of α-W phase which forms definite compounds with refractory elements (Re, Cr, and Mo) diffusing from the alloy during high temperature exposure; and
- the following aluminization step of the protective coating fabrication thanks to its Ni content.

The DB layer formed was then efficient to limit the Al depletion of the coating and to stop the formation of detrimental SRZ, following 50 h of isothermal oxidation at 1100 °C.

In the present paper, the Ni–W based DB was applied between a β-(Ni,Pt)Al bondcoat and a fourth generation Ni-based superalloy. The isothermal and cyclic oxidation behaviours as well as the interdiffusion between the bondcoat and the superalloy were studied for the systems with and without a DB.

2. Experimental

2.1. Substrate material

The fourth generation Ni-base superalloy used for this study is the MCNG (MonoCristal de Nouvelle Géneration) [11]. Its nominal composition is 3.9 wt.% Cr, 1 wt.% Mo, 4.1 wt.% Re, 4.1 wt.% Ru, 5.1 wt.%W, 5.9 wt.% Al, 0.5 wt.% Ti, 5 wt.% Ta, 0.1 wt.% Hf and 0.1 wt.% Si, in a Ni balance, but with several impurities.

Corresponding author.
E-mail address: eric.cavaletti@onera.fr (E. Cavaletti).

2.2. Diffusion barrier fabrication process

The DB system fabrication process is composed of the following steps: (1) Ni–W electrolytic coating is deposited on the superalloy (see [10] for further details); (2) annealed for 16 h at 1100 °C under vacuum (~10^{-6}mbar); (3) a Pt electrolytic coating of 5 μm (±1 μm) is deposited; (4) annealed for 1 h at 1100 °C under vacuum (~10^{-6}mbarr); (5) a low activity vapour phase Al-cementation; (6) annealed for 1 h at 1100 °C under vacuum (~10^{-6}mbarr); and (7) dry grit blasting with corundum.

The fabrication process of the system without a DB comprises only the steps (3) to (7).

2.3. Sample oxidation

Isothermal oxidation tests were performed on as-processed coated specimens in a Setaram TGA24S symmetric thermobalance (1 μg precision) for 100 h in dry synthetic flowing air at 1100 °C and with a heating rate of 60 °C min^{-1}. Mass gain curves were analysed by local fitting to a general parabolic law [12] in order to separate the transient and the stationary kinetics. Low frequency thermal cycling in laboratory air (300 h hot dwells) was conducted by periodic manual removing of specimens from a furnace heated at 1100 °C. Specimens were always cooled down under the same conditions.

2.4. Chemical concentration profiles

The chemical concentration profiles were obtained by EDS microanalysis in SEM. From spectral maps (acquisition of entire spectrum on each pixel), average chemical concentrations are extracted on a line of pixels parallel to the metal/oxide interface, to obtain the concentration profile of the complete system.

3. Results

3.1. As-processed systems characterisation

Fig. 1 shows the microstructure of the as-processed systems with and without a DB. The outer parts of both systems are β-(Ni,Pt)Al. This external layer is 26 μm thick without a DB and 31 μm thick with a DB. The corresponding chemical concentrations profiles are also presented in Fig. 1. They show a slight Al-enrichment and a less critical diffusion of β-like superalloy elements (Cr and Ru) in the coating of the system with a DB.

Between the nickel aluminide coating and the superalloy, the system without a DB (Fig. 1a) presents an interdiffusion zone, IDZ (2), and a continuous SRZ layer (3). The mean SRZ depth (22 μm) corresponds to the Al-diffusion depth in the superalloy. The other system (Fig. 1b) presents a DB layer (2) composed of W-rich precipitates in a β-(Ni,Pt)Al matrix, and an IDZ (3). The Al-diffusion depth into the superalloy of this system is lower than the one of the system without a DB. The system with a DB presents also some isolated SRZ, preferentially formed in dendrite cores of the alloy.

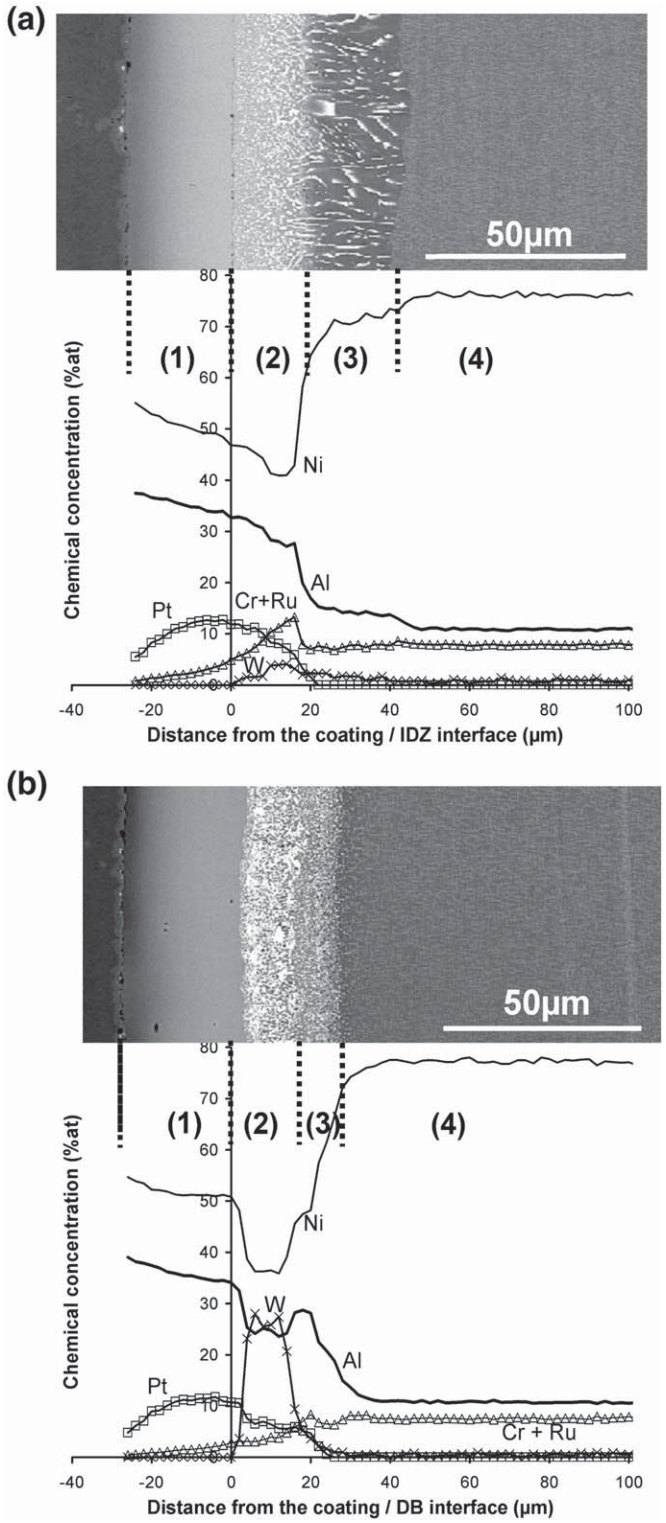

Fig. 1. Microstructure and chemical composition of the as-processed systems without (a) and with a DB (b).

3.2. Oxidation behaviour

3.2.1. Isothermal oxidation kinetics

Thermogravimetric analysis performed during 100 h at 1100 °C shows that both as-processed systems exhibit similar oxidation kinetics and final mass gains. Parabolic coefficients, k_p, calculated after the transient oxidation regime, are equal to 1.3×10^{-7} mg^2 cm^{-4} s^{-1} for the system without a DB and 2.1×10^{-7} mg^2 cm^{-4} s^{-1} with a DB. Both coefficients are very close to the ones found for the kinetics of α-Al_2O_3 growth on pure β-NiAl [13] and slightly higher than the ones measured on a (100) single crystal of β-NiAl and β-NiPtAl [14].

3.2.2. Low frequency cyclic oxidation behaviour

To determine their long term oxidation behaviours, systems with and without a DB have been oxidized for sequential periods of 300 h at 1100 °C under laboratory air up to 1800 h. Corresponding oxidation kinetics are reported in Fig. 2. They confirm the isothermal results showing similar initial oxidation kinetics for both systems, or slightly faster for the DB-base system. But after the second cycle (i.e. 600 h), samples with a DB exhibit a faster decrease of mass corresponding to

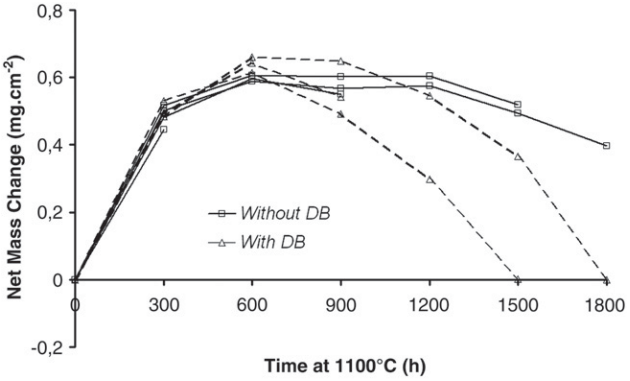

Fig. 2. Net mass change during cycling oxidation at 1100 °C in air (300 h cycles).

slightly more spalling of the oxide scale. This is confirmed by the direct observation of sample surfaces. However, it should be noticed that the mass change difference between the two kinds of samples after 6 cycles (i.e. 1800 h at 1100 °C) is small and about 0.4 mg cm^{-2}.

3.2.3. Evolution of the oxide scale

XRD and SEM analyses (not shown) have demonstrated that after 300 h oxidation at 1100 °C, the oxide scale is entirely composed of α-Al_2O_3, i.e. the metastable θ-Al_2O_3 observed at the external interface after 100 h at 1100 °C is transformed in α-Al_2O_3. After 6×300 h at 1100 °C, the oxide scales of both systems are still mainly composed of α-Al_2O_3. But, Ni-rich spinel oxide formation is also observed, and spinel amount is more significant on systems with a DB. This observation confirms the slightly worse resistance to cyclic oxidation at 1100 °C of the DB-base system.

3.3. Microstructure and chemical concentration evolution during low frequency thermal cycling

3.3.1. Al depletion and phase transformation in the coating

The following phase transformations are induced by oxidation and interdiffusion which cause Al depletion in the coating: β-(Ni,Pt)Al$\rightarrow\gamma'$-$(Ni,Pt)_3Al\rightarrow\gamma$-Ni.

Image analysis on transverse micrographs allowed quantification of the observation that these transformations are delayed in the system with a DB. Fig. 3 shows the microstructures of both systems, without (a) and with a DB (b), after the first 300 h cycle of oxidation at 1100 °C. Both systems exhibit a coating layer composed of β-(Ni,Pt)Al and γ'-$(Ni,Pt)_3Al$ phases. The γ' phase represents, respectively, 70% and 40% of the coating in the system without and with DB.

Fig. 4 shows the evolution of the Al concentration in both systems during this low frequency (long dwell) thermal cycling. The Al concentration is higher in coatings of systems with a DB, at all cyclic oxidation steps.

3.3.2. SRZ propagation

During the first 900 h of oxidation, the SRZ layer follows a parabolic growth kinetic:

$$d_{SRZ}^2 - d_{SRZ0}^2 = k.t$$

with d_{SRZ0} being the initial SRZ depth. The parabolic coefficient k of SRZ propagation is equal to $8.6\cdot10^{-15}m^2\ s^{-1}$ without DB and $7.4\cdot10^{-15}m^2\ s^{-1}$ with a DB. The two parabolic coefficients of SRZ growth are therefore similar and in good agreement with others studies on alloy 5A [4] and TMS-138 [15].

Fig. 3b shows that, in the DB-base system, the originally discontinuous SRZ has become continuous by lateral growth. The white arrow, on Fig. 3b, shows the SRZ initiation zone. These initiation zones lead to coarse formation of TCP phases and precipitation of Ru-rich β-(Ni,Pt)Al (white arrow on Fig. 4b presents the Al enrichment due to this precipitation).

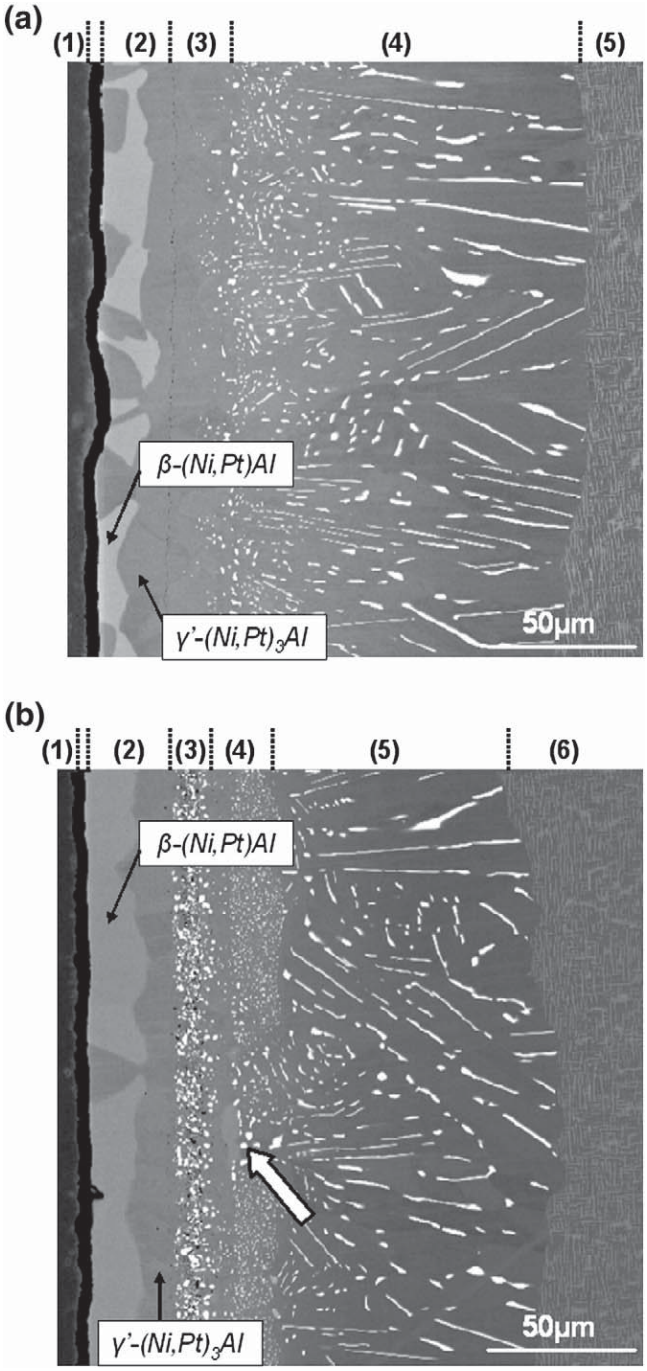

Fig. 3. Microstructure of the systems without (a) and with a DB (b) after 300 h isothermal oxidation at 1100 °C in air.

4. Discussion

4.1. Diffusion barrier influence on oxidation behaviour

EDX analyses (Fig. 4) have shown that the DB-based coating is richer in Al than the coating without a DB, at all steps of low frequency cyclic oxidation. This is well correlated with delayed phase transformations in the coating. As isothermal and cyclic oxidation kinetics are similar or higher for the DB-base system, the observed higher Al

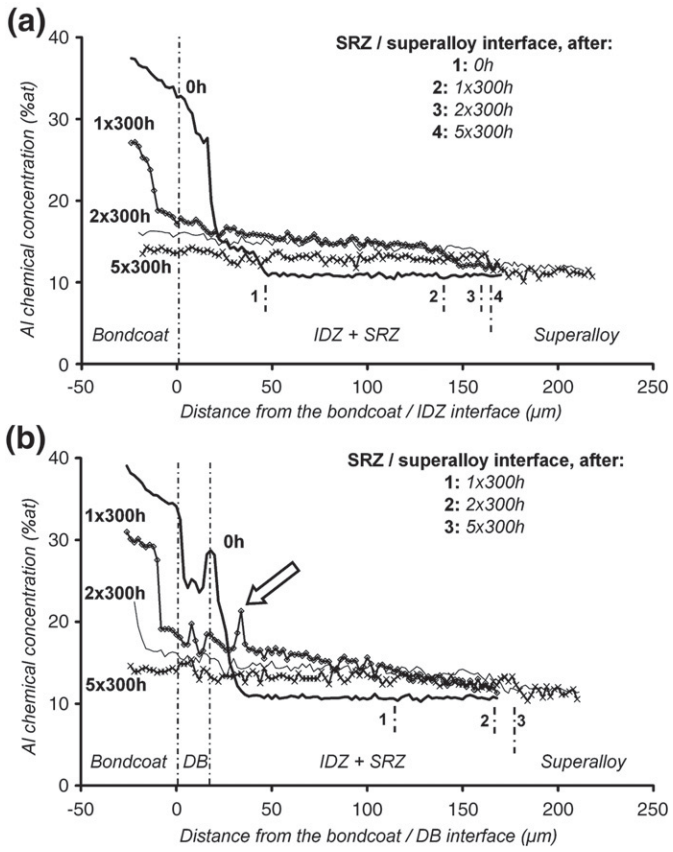

Fig. 4. Evolution of the Al chemical concentration profiles in systems without (a) and with a DB (b) following cyclic oxidation at 1100 °C in air.

content in this system is certainly due to the W-rich precipitates layer acting as a DB and limiting the Al depletion of the coating.

Despite its higher Al content, the system with DB exhibits a slightly worse oxidation behaviour than the system without a DB. Two reasons may explain this observation. Firstly, some S enrichment was detected by GDMS analysis (concentration profiles mode) in the as-processed system with a DB. A local S enrichment up to 22 wt-ppm over 15 µm was measured in the middle of the DB layer. For comparison, the maximal S concentration in the system without DB was 2 wt-ppm. This S enrichment, due to the Ni-W coating step for which $NiSO_4$ salts are used, is known to have detrimental influence on oxide scale adherence [16]. Secondly the γ′-$(Ni,Pt)_3Al$ and γ-Ni phases of the DB-based coating are enriched in W due to the dissolution of the W comprised in the DB layer, W has a higher solubility limit in γ′ and γ than in the original β phase of the coating [17]. After 5×300 h of oxidation, both systems present coatings composed of γ′ and γ phases, and the mean W concentrations in these phases are, respectively 2.8 at.% and 5.0 at.% with the DB, and 0.9 at.% and 0.8 at.% without DB. This W enrichment can lead to a lower adherence of the alumina oxide scale [18].

4.2. Diffusion barrier influence on SRZ formation and propagation

Instead of forming a continuous SRZ layer beneath the IDZ, the as-processed system with a DB presents some isolated SRZ formation. These SRZs are localised to the dendrite cores of the alloy, which are Re, W and Ru enriched zones of third and fourth generation superalloys. These elements are all γ-like elements, so dendrite cores are the zones within the superalloy where the γ phase is the most supersaturated. Because SRZs are formed by discontinuous precipitation, for which supersaturation is a driven force [19], dendrite cores are prone to initiate SRZ [5,20].

During long term cyclic oxidation treatments, it was shown that SRZ propagation follows similar parabolic kinetics for both systems. This means that DB addition only delays SRZ formation but does not slow down its propagation. The propagation kinetics measured in our study are in good agreement with those measured by others on different systems [4,15], and are also very close to the interdiffusion coefficient in the γ′-Ni_3Al phase ($6 \cdot 10^{-15} m^2\ s^{-1}$ [21] or $1 \cdot 10^{-14} m^2\ s^{-1}$ [22]). Then, it seems that SRZ propagation is controlled by interdiffusion in the alloy matrix.

4.3. Influence of SRZ formation on bondcoat Al depletion

Fig. 5 shows the Al chemical concentration profiles in zones with and without SRZ formation after 300 h of oxidation at 1100 °C. It is clear that the lower Al diffusion into the superalloy in the zone without SRZ formation permits to keep a higher Al content in the coating.

5. Conclusions

A DB layer based on a Ni–W electrolytic coating has been developed between a fourth generation superalloy and a Pt-modified nickel aluminide protective coating. The addition of this layer leads to the following consequences:

1- On as-processed system, the Ni–W coating leads to the formation of a DB layer composed of a dense α-W precipitation in a β-(Ni,Pt)Al matrix. This layer acts like a DB by limiting the superalloy element (Ru and Cr) diffusion from the alloy to the coating, and also by limiting the formation of the detrimental SRZ. In this system, SRZs are discontinuous beneath the IDZ and localised in dendrite cores of the alloy.
2- During low frequency (long dwell) thermal cycling at 1100 °C, the DB layer limits the Al depletion of the coating, which leads to delayed phase transformation.
3- Despite the efficiency of the DB layer in limiting substrate element movement, the system cyclic oxidation behaviour is degraded as shown by a larger extent of oxide scale spallation. The system with the DB also tends to form more Ni-rich spinel oxide after prolonged exposure at 1100 °C. These differences could be explained by the observed increased pollution in S during the Ni–W coating step and/or by the dissolution of the W comprised in the DB in the γ′-$(Ni,Pt)_3Al$ and γ-Ni phases of the coating.
4- SRZ propagation kinetics are similar with and without a DB. After high temperature exposure, the SRZs formed in the system with DB, which were originally discontinuous, become continuous by lateral growth, thus the DB delays the formation of a SRZ.
5- SRZ formation influences the Al diffusion towards the superalloy. In addition to its detrimental influence on mechanical properties, it

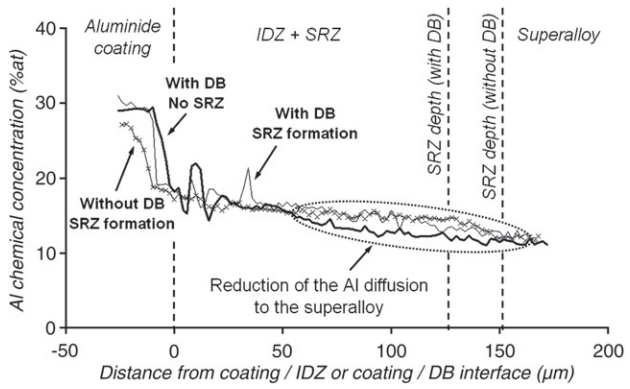

Fig. 5. Comparison between Al chemical concentration profiles obtained in zones containing SRZ and in zones without SRZ formation after 300 h isothermal oxidation at 1100 °C in air.

has been shown that SRZ formation contributes also to the Al depletion of the coating.

References

[1] M. Göbel, A. Rahmel, M. Schütze, M. Schorr, W.T. Wu, Mater. High Temp. 12 (4) (1994) 301.
[2] Y. Zhang, J.A. Haynes, B.A. Pint, I.G. Wright, W.Y. Lee, Surf. Coat. Tech. 163–164 (2003) 19.
[3] M.W. Chen, M.L. Glynn, R.T. Ott, T.C. Hufnagel, K.J. Hemker, Acta Mater. 51 (2003) 4279.
[4] W.S. Walston, J.C. Schaeffer, W.H. Murphy, in: R.D. Kissinger, D.J. Deye, D.L. Anton, A.D. Cetel, M.V. Nathal, T.M. Pollock, D.A. Woodford (Eds.), Superalloys, The Minerals, Materials and Metals Society, Warrendale, PA, 1996, p. 9.
[5] O. Lavigne, C. Ramusat, S. Drawin, P. Caron, D. Boivin, J.-L. Pouchou, in: K.A. Green, T.M. Pollock, H. Harada, T.E. Howson, R.C. Reed, J.J. Schirra, S. Walston (Eds.), Superalloys, The Minerals, Materials and Metals Society, Warrendale, PA, 2004, p. 667.
[6] J. Müller, M. Schierling, E. Zimmermann, D. Neuschütz, Surf. Coat. Tech. 120–121 (1999) 16.
[7] J.A. Haynes, Y. Zhang, K.M. Cooley, L. Walker, K.S. Reeves, B.A. Pint, Surf. Coat. Tech. 188–189 (2004) 153.
[8] T. Narita, F. Lang, K.Z. Thosin, T. Yoshioka, T. Izumi, H. Yakuwa, S. Hayashi, Oxid. Met. 68 (2007) 343.
[9] M.P. Bacos, P. Josso, FR Patent 2881439. (2006).
[10] E. Cavaletti, S. Mercier, D. Boivin, M.P. Bacos, P. Josso, D. Monceau, Mater. Sci. Forum 595–598 (2008) 23.
[11] P. Caron, J.L. Raffestin, FR Patent 2780982. (2000).
[12] D. Monceau, B. Pieraggi, Oxid. Met. 50 (1998) 5.
[13] M.W. Brumm, H.J. Grabke, Corros. Sci. 33 (1992) 1677.
[14] Y. Cadoret, D. Monceau, M.P. Bacos, P. Josso, V. Maurice, P. Marcus, Oxid. Met. 64 (2005) 185.
[15] Y. Matsuoka, Y. Aoki, K. Matsumoto, T. Suzuki, K. Chikugo, K. Murakami, in: K.A. Green, T.M. Pollock, H. Harada, T.E. Howson, R.C. Reed, J.J. Schirra, S. Walston (Eds.), Superalloys, The Minerals, Materials and Metals Society, Warrendale, PA, 2004, p. 637.
[16] J.A. Haynes, M.J. Lance, B.A. Pint, I.G. Wright, Surf. Coat. Tech. 146–147 (2001) 140.
[17] C.C. Jia, K. Ishida, T. Nishizawa, Metall. Mater. Trans. A 25 (3) (1994) 473.
[18] M.E. El-Dahshan, D.P. Whittle, J. Stringer, Corros. Sci. 16 (2) (1976) 83.
[19] B.E. Sundquist, Metall. Trans. 4 (1973) 1919.
[20] D.K. Das, K.S. Murphy, S. Ma, T.M. Pollock, Metall. Mater. Trans. A 39 (2008) 1647.
[21] T. Ikeda, A. Almazouzi, H. Numakura, M. Koiwa, W. Sprengel, H. Nakajima, Acta Mater. 46 (15) (1998) 5369.
[22] M. Watanabe, Z. Horita, M. Nemoto, Defect Diffus. Forum 143 (1997) 147.